



Please cite the Published Version

De Chowdhury, S, Causon, D, Qian, L , Mingham, C, Chen, H, Lin, Z, Zhou, Jian Guo , Pullen, T, Silva, E, Hu, K, Russell, M, Manson, S, Winter, H, Joly, A, Stewart, D and Wood, M (2019) Investigation of Wind Effects on Wave Overtopping at Sea Defences. In: Coastal Structures 2019, 30 September 2019 - 02 October 2019, Hannover, Germany.

DOI: https://doi.org/10.18451/978-3-939230-64-9_084

Publisher: Bundesanstalt für Wasserbau

Downloaded from: <https://e-space.mmu.ac.uk/624558/>

Usage rights:  [Creative Commons: Attribution 4.0](https://creativecommons.org/licenses/by/4.0/)

Additional Information: Copyright Bundesanstalt für Wasserbau

Enquiries:

If you have questions about this document, contact openresearch@mmu.ac.uk. Please include the URL of the record in e-space. If you believe that your, or a third party's rights have been compromised through this document please see our Take Down policy (available from <https://www.mmu.ac.uk/library/using-the-library/policies-and-guidelines>)

Conference Paper, Published Version

De Chowdhury, S.; Causon, D.; Qian, L.; Mingham, C.; Chen, H.; Lin, Z.; Zhou, J. G.; Pullen, T.; Silva, E.; Hu, K.; Russel, M.

Investigation of Wind Effects on Wave Overtopping at Sea Defences

Verfügbar unter/Available at: <https://hdl.handle.net/20.500.11970/106700>

Vorgeschlagene Zitierweise/Suggested citation:

De Chowdhury, S.; Causon, D.; Qian, L.; Mingham, C.; Chen, H.; Lin, Z.; Zhou, J. G.; Pullen, T.; Silva, E.; Hu, K.; Russel, M. (2019): Investigation of Wind Effects on Wave Overtopping at Sea Defences. In: Goseberg, Nils; Schlurmann, Torsten (Hg.): Coastal Structures 2019. Karlsruhe: Bundesanstalt für Wasserbau. S. 841-850.
https://doi.org/10.18451/978-3-939230-64-9_084.

Standardnutzungsbedingungen/Terms of Use:

Die Dokumente in HENRY stehen unter der Creative Commons Lizenz CC BY 4.0, sofern keine abweichenden Nutzungsbedingungen getroffen wurden. Damit ist sowohl die kommerzielle Nutzung als auch das Teilen, die Weiterbearbeitung und Speicherung erlaubt. Das Verwenden und das Bearbeiten stehen unter der Bedingung der Namensnennung. Im Einzelfall kann eine restriktivere Lizenz gelten; dann gelten abweichend von den obigen Nutzungsbedingungen die in der dort genannten Lizenz gewährten Nutzungsrechte.

Documents in HENRY are made available under the Creative Commons License CC BY 4.0, if no other license is applicable. Under CC BY 4.0 commercial use and sharing, remixing, transforming, and building upon the material of the work is permitted. In some cases a different, more restrictive license may apply; if applicable the terms of the restrictive license will be binding.



Investigation of Wind Effects on Wave Overtopping at Sea Defences

S. De Chowdhury, D. Causon, L. Qian, C. Mingham, H. Chen, Z. Lin & J. G. Zhou
Manchester Metropolitan University, Manchester M1 5GD, UK

T. Pullen & E. Silva
HR Wallingford, Wallingford OX10 8BA, UK

K. Hu
Royal HaskoningDHV, Harlands Road, Haywards Heath RH16 1PG

M. Russell & S. Manson
Environment Agency, Horizon House, Deanery Road, Bristol, BS1 5AH, UK

H. Winter & A. Joly
EDF Energy R&D UK Centre, Interchange, 81-85 Station Road, Croydon CR0 2RD, UK

D. Stewart & M. Wood
Torbay Council, Torquay TQ2 5QW, UK

Abstract: Quantitative assessments of wind effects on wave overtopping are carried out using CFD simulations with the open source solver OpenFOAM. The desired wind speeds are achieved efficiently by introducing artificial pressure gradient terms for desired zones inside the computational domain. A new run-time post processing utility has been developed to track the overtopping water over a sea defence. Numerical results are validated using (1) a past experimental study with simple sloped defence and (2) new experiments that were conducted at HR Wallingford with a more realistic structure. Several additional calculations with both small and large water depths reveal that with a high wind speed the overtopping volume can be increased by 30% compared to that without wind. The 2D code is then extended to wave overtopping at a semi-circular beach in the plane as a hypothetical 3D sea defence in order to investigate the 3D effect of wind speeds.

Keywords: wave overtopping, wind effect, wind waves, wave structure interactions, 3D effect

1 Introduction

Many coasts are vulnerable to wind from moderate to very high wind speeds during normal weather as well as a storm surge. Coastal defences are standard choices to protect the coasts against flooding from wave overtopping and yet still it is not usual to design them based on studies specifically focused on an understanding of the wind effects. The primary reason is that incorporation of a wind generation facility into an existing physical flume is not straightforward and the scaling laws for wind effects are unknown. Thus, coastal engineers are left with prescribing a wide margin for coastal defence-height which is seldom found and less economical in practice.

The topic of wind wave interactions is rather well studied (see for example, Miles (1957); Kharif et al. (2008); Chalikov (1978); Yan and Ma (2010); Xie (2014); Hasan et al. (2018) etc) and the problem of wind effects on wave overtopping can be thought of, in a sense, as a special class of the wind wave interaction problem. There are several mechanisms through which wind contributes to overtopping: (1) wind energy transfer to the waves in between successive run-ups; (2) curvature of overshooting water due to the strong shear force from the wind after a strong wave impact and (3) wind driven surface currents in shallow waters. Mechanism (1) is mostly found in the case of a mildly sloping or curved structure, whereas, for a vertical seawall causing strong reflection of the incident waves, mechanism (2) is dominant. There are a few studies (for example see Ward et al. (1996, 1998)) which focused on (1) where in some cases wind effects on run up and overtopping on slopes are clearly

visible, especially at high wind speeds. Mechanism (2) by its nature leads to more violent wave structure interactions than the others and this is where we put the focus in this paper. Firstly, we describe the numerical model and discuss the methodologies adopted to introduce the desired wind speed into the computational model. Then we discuss the basis for choosing the parameters for the incident wave conditions. Two set of tests are reproduced in order to validate the numerical calculations: the first one is that reported in Ward et al. (1996) and the second one is a new series of tests conducted recently at the Froude Laboratory in the flume at HR Wallingford, UK. Although it is difficult to retain a steady wind in the physical model tests due to the limitations of the facility, wind effects on wave overtopping are clearly noticeable. Because of this, we focus on the physical test results without wind speed, which are applied to validate the numerical model. Secondly, many numerical simulations are conducted where we change the incident wave heights, period and sea-bed slope for three different wind speeds to quantify the effect of wind speed on wave overtopping at a vertical seawall with a fixed freeboard. Finally, we describe a 3D test with a hypothetical island in order to investigate the 3D flow features under a given wind speed.

2 Numerical modelling with OpenFOAM

We use an open source numerical model named OpenFOAM in order to simulate wind effects on wave overtopping. OpenFOAM solves the following the Reynolds-averaged Navier–Stokes (RANS) equations using a Finite Volume Discretization of a domain:

$$\nabla \cdot \mathbf{U} = 0, \quad (1)$$

$$\frac{\partial \rho \mathbf{U}}{\partial t} + \nabla \cdot (\rho \mathbf{U}) \mathbf{U} - \nabla \cdot \mu \nabla \mathbf{U} = -\nabla p^* - \delta(\nabla p^*) - (\mathbf{g} \cdot \mathbf{R}) \nabla \rho, \quad (2)$$

where, \mathbf{U} is the velocity field and \mathbf{R} is the position vector in a Cartesian Coordinate System. The pseudo dynamic pressure p^* is the total pressure minus the hydrostatic pressure. ρ is the density, μ is the coefficient of dynamic viscosity and $\mathbf{g} = 9.81 \text{ m/s}^2$ is the acceleration due to gravity. The desired mean wind speed (\bar{U}) is introduced through the additional pressure gradient correction term $\delta(\nabla p^*)$ over prescribed cell zones by

$$\delta(\nabla p^*) \leftrightarrow \frac{\sum_i \left(\frac{\bar{U}}{|\bar{U}|} \mathbf{U}_i \right) V_i}{\sum_i V_i}, \quad (3)$$

where, \mathbf{U}_i is the velocity at the i^{th} cell and V_i is the volume of this cell. This correction is applied only to a few selected cells adjacent to the coastal defence. This is achieved using the "fvOptions" framework with the option named "meanVelocityForce" in OpenFOAM. This framework mimics certain features in the flow which are the outcome of a more complex process, e.g. introducing high momentum flux in the air through a turbine rotating at moderate to high speed (see the report by Capitao (2017)). This approach helps to avoid a very small time step for a stable Courant no ($O(0.5)$). The interface between the air and water is captured by using the Volume Of Fluid (VOF) technique by solving the following equation for phase fraction (α)

$$\frac{\partial \alpha}{\partial t} + \nabla \cdot (\mathbf{U} \alpha) + \nabla \cdot \mathbf{U}_c \alpha (1 - \alpha) = 0, \quad (4)$$

where, $|\mathbf{U}_c| = \min(c_\alpha |\mathbf{U}|, \max(|\mathbf{U}|, 0))$ and the quality of the interface is maintained by the factor c_α . The fraction α is bounded within $[0,1]$ with value 0 referring to a dry cell and 1 to a wet cell. Any value within the range refers to a cell at the air-water interface. The spatial terms are discretized with a combination of central difference and upwind schemes. The solution is marched in time with a standard first order Eulerian scheme.

For a water wave simulation one key issue is wave generation at the inlet and its absorption at the outlet for carrying out simulations for a sufficiently long time. In the present study, we use the set of libraries named olaFlow (Higuera et al. (2013)). In some cases where wave conditions are not

necessarily shallow, we use waves2Foam instead (Jacobsen et al. (2012)). This increases the computational time and we have to use relaxation zones in addition to the desired domain, which gives very good absorption of the outgoing waves and scope to conduct a proper spectral analysis of the steady state waves. Such implementations are necessary to find the growth in the incident wave amplitude due to a wind speed. All the simulations are performed using the OpenFOAM ESI version 1706.

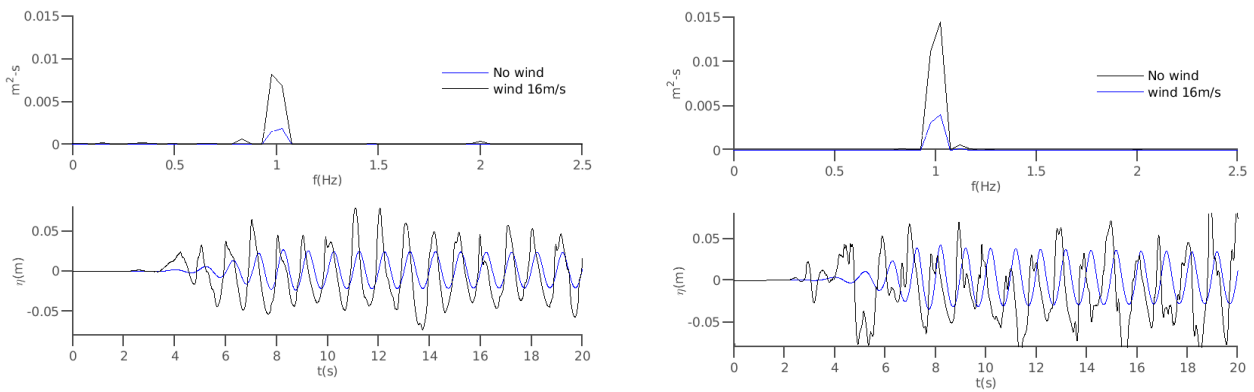
2.1 Development of a new run-time post processing utility for tracking overtopping

The wave overtopping is highly localized in time and thus it is ideal to measure it during the actual running of the main solver (equations (1)-(4)). The function object in waves2Foam library named "overtopping" (Jacobsen (2017)) precisely does this task by calculating the volume fluxes of the water phase over selected zones of cell faces and then summing over these to get the overtopping in a given direction. However this function object only works with certain specific foam-extend versions (i.e., 3.2) and it is not straightforward to be generalised for any OpenFOAM version (e.g., ESI v1706) due to different naming conventions used for C++ function variables in foam-extend versions. A close inspection of the native runtime post processing function in ESI versions reveals that the function object named "fluxSummary" contains many similar classes and variables as in "overtopping" and any member functions can be implemented within "fluxSummary" using these variables or derived from them if not present already. We found that this implementation inside "fluxSummary" yields results very close to that of "overtopping" and henceforth we always refer to it as "fluxSummaryNew" for calculating wave overtopping.

3 Validation Tests

3.1 Ward et al. (1996)

The initial tests we consider to check the reliability of our numerical simulations are based on a previous study by Ward et al. (1996). These tests consist of setting up a numerical wave tank 28m in length with a water depth of 0.5m. The ceiling of the flume is 0.41m above mean water level. Two set of tests were conducted: one without any structure with fixed depth maintained throughout the tank and another with a 1:3 slope located near the outlet to consider overtopping. The overtopping water was collected in a tank behind the sloping structure as that in the original experiments and we track the overtopping water just at the entry to this tank in our numerical simulations. The incident wave is defined as a regular monochromatic wave of period 1s. The desired wind speed in the experiments was achieved by an air intake-blower combination and initially we look into the effects of wind speed on the growth of the incident wave energy as shown in Fig. 1.



a) Wave energy spectra with and without wind for wave height 0.05m

b) Wave energy spectra with and without wind for wave height 0.075m

Fig. 1. Wave energy growth due to wind speed.

The bottom panel in Fig. 1a shows the wave elevation time history measured at 4m from the inlet without and with a wind speed of 16m/s. In the presence of the high wind speed there is significant amplification of the wave envelope and this is reflected in the wave energy distributions over all frequencies (top panel Fig. 1a). However, with higher wave height (i.e., 0.075m) at the inlet, the situation is more complicated (Fig. 1b). In this case there is greater modulation of the wave profile by the wind due to the higher wave height at the inlet and this leads to both very high frequency (short-lived) and strongly nonlinear waves. This is evident in the wave elevation time history in the bottom panel of Fig. 1b. Unlike the smaller input wave height of 0.05m (i.e., top panel Fig 1a), the energy in the wave in the presence of wind speed is distributed over numerous subharmonics. We make a linear superposition of all the energy distributions in various other frequencies at the peak frequency and obtain the final distribution as shown in the top panel in Fig. 1b. For these two wave heights we found that the amplification due to wind is very close to that reported by Ward et al. (1996).

The purpose of these tests is to design a proper input signal to the wave maker replicating the wind effects and then use them to study the wind effects on wave overtopping. This is presented in Fig. 2. Here, we compare the predictions of the numerical calculations using OpenFOAM (OF) and the developed utility "fluxSummaryNew" with those measured in the experiments (Exp) by Ward et al. (1996). We used a fixed crest elevation (C_{eq}) and vary the wave heights (H) accordingly in the range shown. The numerical calculation is found to agree very well with these measurements. It shows that at higher (C_{eq}/H) ratio, i.e., from 0.7 onwards, the effects of wind speed are much significant on overtopping than that at a lower ratio, which can be as high as up to more than twice the overtopping volume accumulated without wind.

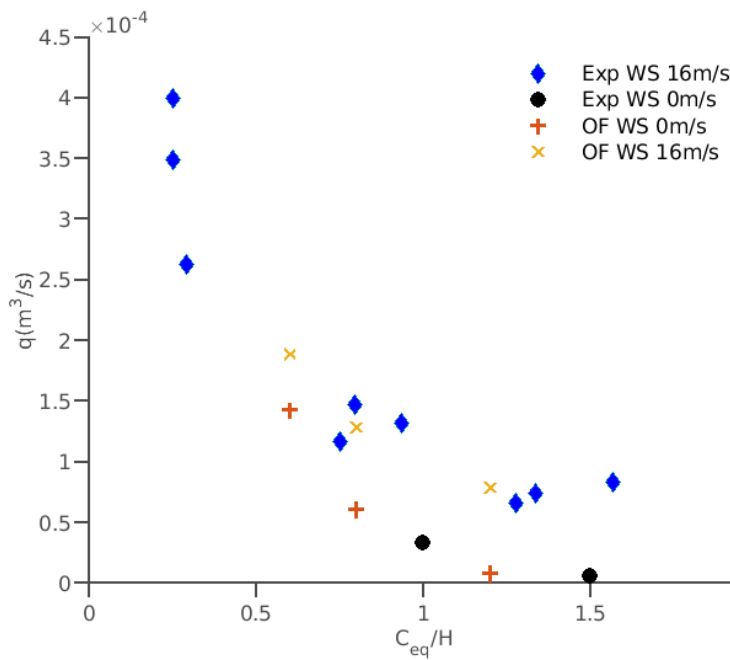


Fig. 2. Comparison of wave overtopping rate per unit crest width for various incident wave heights.

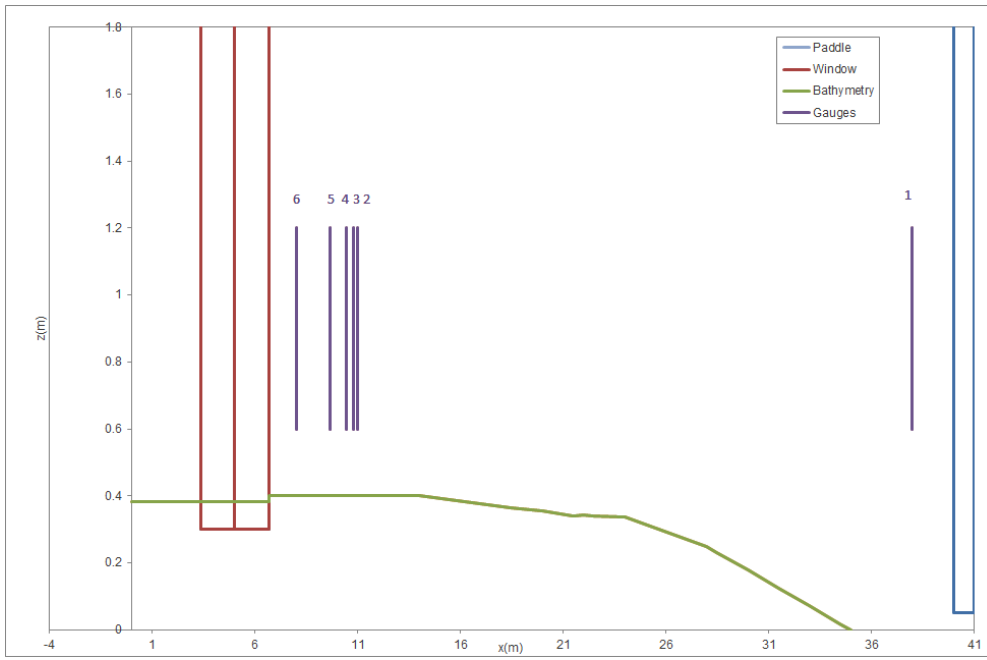
It should be noted here that in our simulations while we want to find the growth in wave amplitude due to wind using energy spectra, we use waves2Foam for wave generation and absorption, whereas, when we want to measure the overtopping, we use olaFlow since it supports active wave absorption at the inlet to minimize wave reflection from the sloping structure.

3.2 Experiments conducted at HR Wallingford

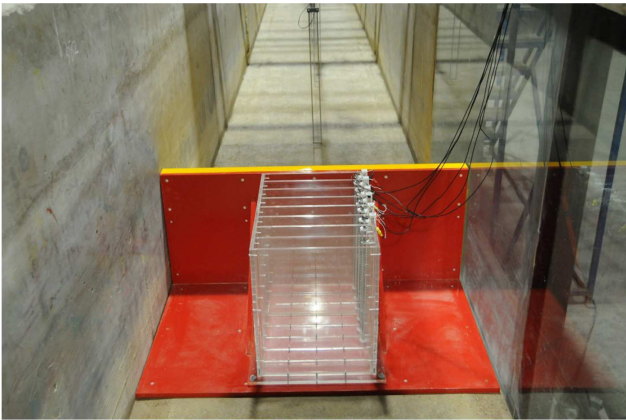
Recently we have conducted a series of tests in the physical flume at the laboratory of HR Wallingford to investigate wind effects on wave overtopping. The model flume bathymetry is shown in Fig. 3a. with a scale of 1:17 of the actual prototype. Here we have used a vertical structure with a very steep front slope as a sea defence. Random waves are used as incident waves by the wave making system at the inlet in order to get statistically significant results. The data is processed based on one thousand waves generated in a typical run of 2000s of physical time. The incident wave spectra is distinguished from that of reflected waves based on the wave elevation measurements at gauges 2-5 using the methodology of Isaacson (1991). This incident wave spectra is then used in the numerical wave tank to create the desired wave conditions at the coastal defence. The overtopping water is collected in a tank just located behind the structure (Fig. 3b) and the water level rise during the overtopping cycles is monitored using six dip sticks in the corresponding separated chambers (which are not connected with each other) in the tank for collecting overtopping water as shown in Fig. 3c. This enables us to measure the distribution of overtopping water from the sea defence, and the excess water is taken out by means of pumps when the tanks get full during the tests and duly considered in the final evaluation of the overtopping rate. Two rows, each containing two fans are placed in front of the defence and create a wind field when we want to measure the effects of wind on overtopping. The fans are driven with a specific power input (set by dials) related to the constant wind speed in the physical model, which represents qualitatively some observed at the coastal defence due to scale difficulty in the physical test. Our choice for the water depth (h), spectral wave height (H_{m0}) and the offshore water wave length ($L_{m-1,0}$) (see EurOtop manual (2018) for definition of these parameters) at the structure is guided by the following condition on the impulse parameter

$$\frac{h^2}{H_{m0}L_{m-1,0}} \leq 0.23. \quad (5)$$

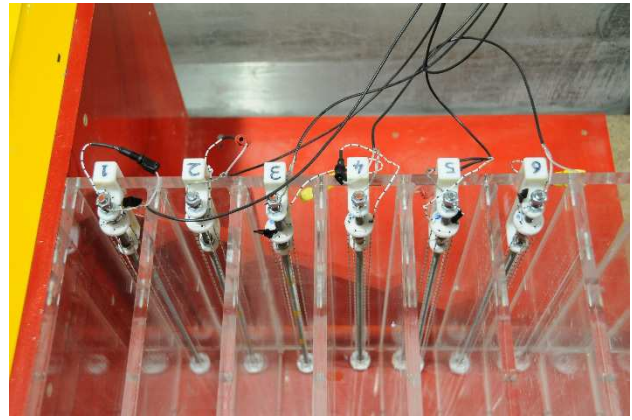
We find that while this parameter is at relatively low value ($O(0.1)$), we have a very strong overshoot of the waves immediately after the impact on the structure. In the presence of a strong wind, most of this overshooting water which would otherwise fall back to the water is now blown over the structure. When the overshoot is preceded by plunging type breaking just before impact then it is characterized by stronger 3D effects (the continuous fluid stream is broken into many smaller droplets) than that without breaking. The equivalent flow features are also verified in the numerical simulations and this is seen when we compare the distribution of the overtopping water in the tank as shown in Fig. 4, with the breadth (all same) of the compartments as shown in Fig. 3b. The width (perpendicular to the plane of the paper) of the tank is 0.376m. The highest overtopping in the first tank is due to the falling of this large volume of overshooting water under the action of gravity.



a) Details of the flume bathymetry



b) Arrangement of the tank for collecting overtopping water.



c) Arrangement of dip sticks to measure overtopping.

Fig. 3. Details of the physical flume at HR Wallingford.

The impulse parameter achieved in this case in the experiment was 0.085 and in the numerical simulation is found to be 0.06. The overtopping in the first tank is under predicted by 20% which might be due to the aforementioned 3D effects which are not well resolved in 2D numerical simulations. Other than that the observed overtopping is found to undergo a very sharp decrease after the second tank (i.e., around 0.2m) onwards both in the numerical simulations and in the experiments. The processing of the data for producing similar results for a given wind speed is still under progress and will be reported when available.

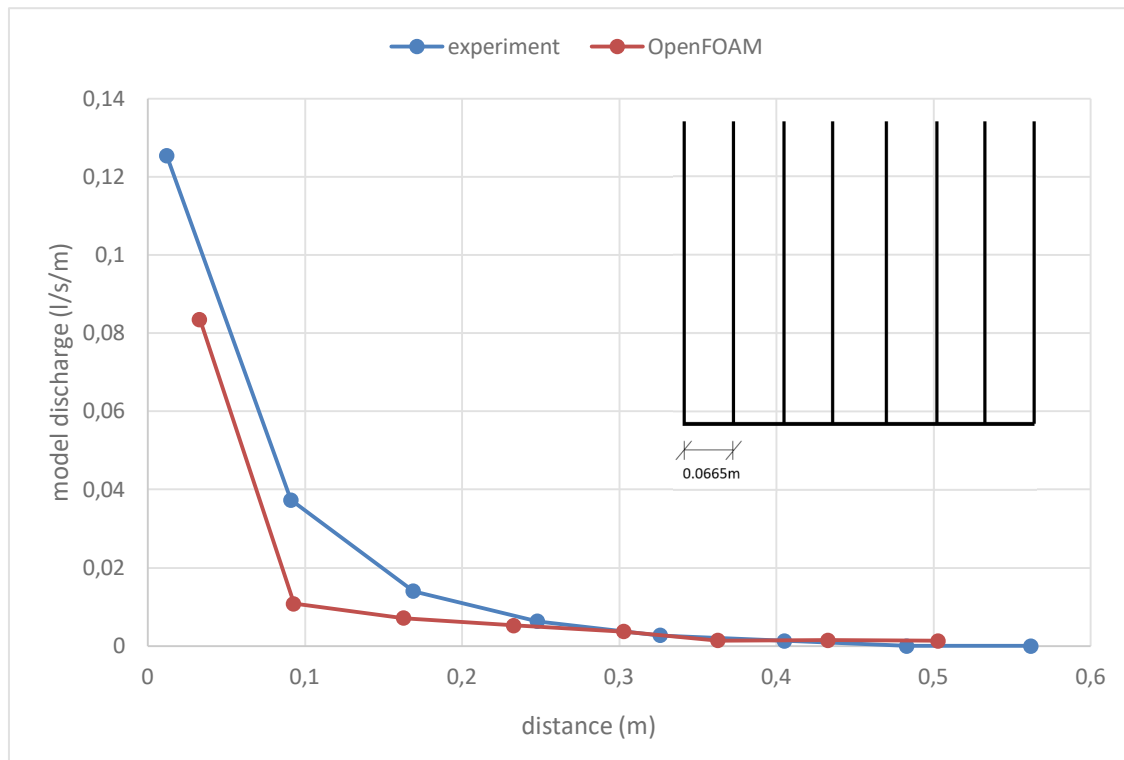


Fig. 4. Comparison of the overtopping distribution over distance from the sea defence.

4 Illustrative calculations for wind effects on overtopping

We have conducted a series of additional tests with the numerical model to create a comprehensive database for accessing wind effects on wave overtopping. In this section we provide a brief background to these tests to quantify wind effects on overtopping.

4.1 2D simulations

The 2D simulations are conducted in a Numerical Wave Tank with a water depth of 10m. We use a vertical wall as a model for the sea defence and this structure is located at the top of a given slope. For this set up we have recently carried out a number of simulations for different incident wave heights, periods; front slopes, sea defence, free boards and wind speeds. Here, we only present results for the case where we use a regular monochromatic cnoidal wave of height 3.5m; wave period 8s and slope 0.16. The impulse parameter for this case is found to be 0.2. The time history of the overtopping flux measured during the simulations are shown in the top panel of Fig. 5. Here the wind speeds are introduced only after the first overtopping cycle (i.e., after 30s) in order to achieve similar wave reflections at the structure in all simulations. The bottom panel is the time averaged overtopping over cycles. We provide the results further in Table 1 for the purpose of quantification. We only consider the data after 70s when the variation in the overtopping rate is close to a steady state.

Tab. 1. Variation in the overtopping with change in wind speeds

Wind speed	0	25m/s	30m/s	50m/s
Overtopping (m^3/sm)	0.0138	0.0181	0.0211	0.035

Wind effects on wave overtopping for the speeds in the range 20-50m/s are given in Table 1, from which we find that the overtopping is increased by almost 31% for a wind speed of 25m/s compared to that without any wind speed.

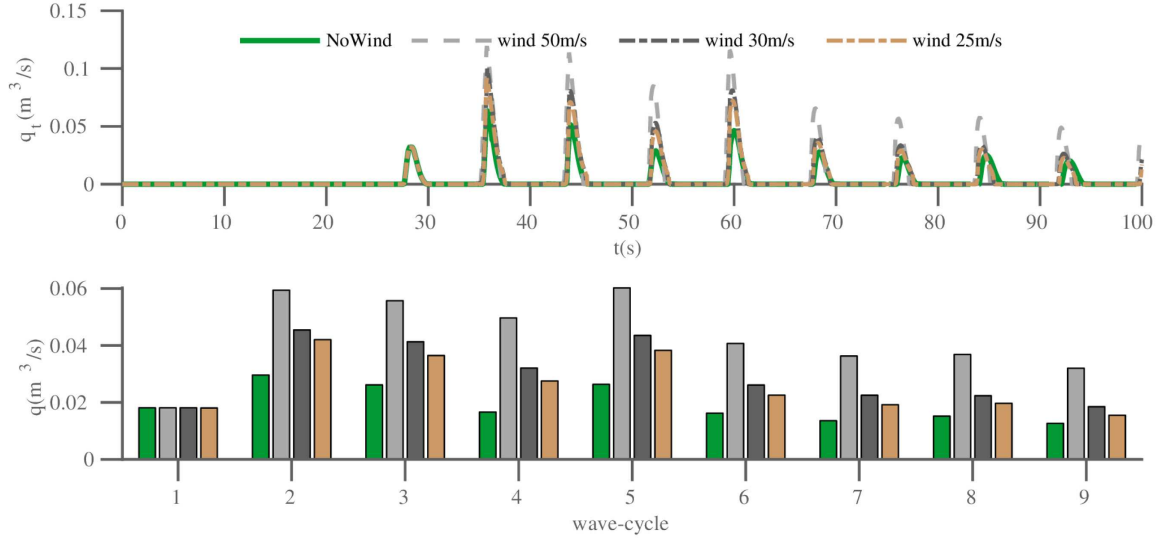


Fig. 5. Overtopping time history due to a given regular wave incidence at a vertical sea wall.

4.2 3D Simulations

In order to gain further insight into the wave structure interaction process, we have also extended the 2D simulations above to the case with a 3D structure for the same height, base and slope as in the 2D structure. The 3D structure can be thought as a model of an island with a semi-circular beach profile. The geometry of this structure is shown in Fig. 6, which is highly simplified 3D structure in reality.

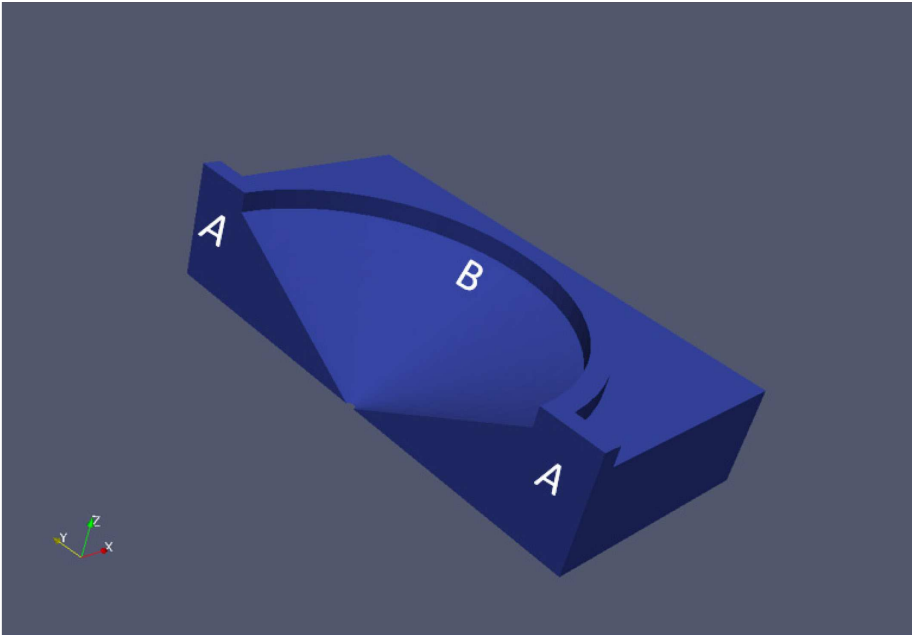


Fig. 6. 3D geometry used as a model of a hypothetical semi-circle island with radius of 18.5m and same 2D slope.

The effect of the impulse parameter (see equation (5)) in enhancing the overshoot is clearly visible in Fig. 7. Near the entry of the island (zones A in Fig. 6) where there are no slopes, the water depth is the same as that in offshore and the impulse parameter is high. On the other hand, as the incoming waves enter into the semi-circular region over the given slope, there is a gradual decrease in water depth and the impulse parameter becomes much lower than the limit in equation (5). Also a very minor reflection in this location (zone B in Fig. 6) and higher overshoot than that near the entry is observed (Fig. 7a). Under the same incident wave conditions as used in our 2D simulations above, we find that there is around an 8% increase in the height of the overshoot at the seawall in the 3D simulations.

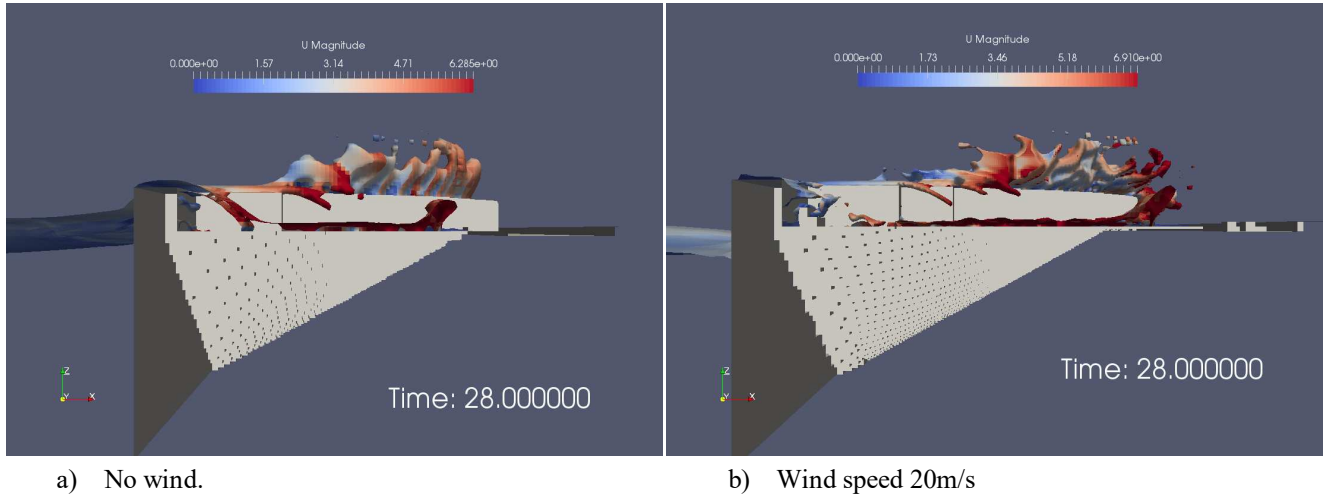


Fig. 7. Wave interaction with the vertical seawall in 3D with and without wind effects.

Next, we have selected a number of cell zones above the vertical structure covering the entire semi-circular beach profile and introduce a wind speed of 20m/s after some overtopping cycles. Due to the presence of this strong wind, the overshooting water at the same time step as in the previous case now tends to curve towards the island (Fig. 7b). We find from our numerical simulations that the degree of curvature is strongly dependent on the wind speed and might not be very evident at relatively lower wind speed, i.e., $O(10-15\text{m/s})$ at the water depth considered. The effect of curvature due to the wind is the cause of greater wetting of the land area behind the seawall and this is shown in Fig. 8.

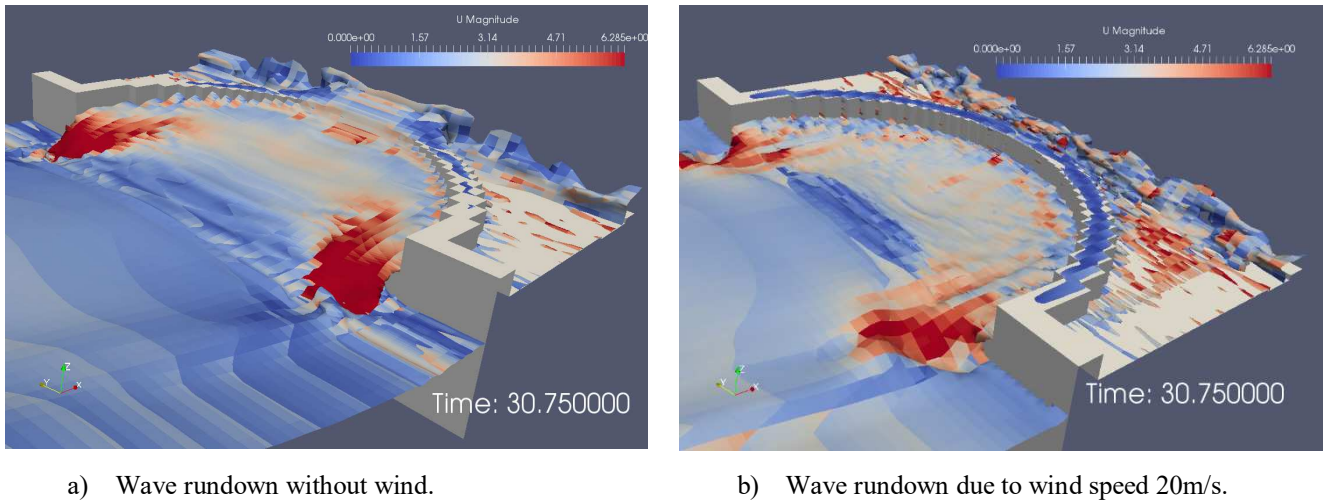


Fig. 8. Overtopping and rundown over an island with and without wind.

The overshooting water during the overtopping recesses back to the sea with a very high velocity under the action of gravity (Fig. 8a). Whereas, in the presence of a strong wind, the continuous falling stream disintegrates into two fluid masses: one that falls back to the sea as before, but another continues to move towards the land area above the seawall (Fig. 8b). Subsequently this new fluid mass is blown landward and causes greater overtopping. Due to loss of this component of the fluid body, the recessing water has a lower momentum in the presence of wind than that without wind.

We also have the capability to change the wind direction with respect to the incident wave direction and measure the overtopping in any given direction. Thus, we can generate rose diagrams for overtopping volumes under a wide range of wave and wind conditions.

5 Conclusions

We have developed a set of strategies and tools for carrying out efficient numerical simulations to investigate wind effects on wave overtopping based on the open source CFD model OpenFOAM. The calculations are validated both with a past study and a series of new tests carried out at HR Wallingford. We have been able to determine the amplification in the incident wave amplitude due to wind and with that information we are able to predict overtopping close to that measured in the experiments. From the numerical tests we have found that under the action of moderate wind speeds, the overtopping can be as high as up to 30% more than that without wind speed. Past studies revealed that it is difficult to scale wind effects on wave overtopping since waves of different period and heights get modulated differently under a given wind speed and in some cases wave overtopping is found to be as high as 50% greater than that without wind. This suggests that the results from the present studies are comparable in scale to those of past studies. The 3D simulations yields higher overshoots compared to 2D simulations under the same incident wave conditions and gives results very close to a violent wave interaction with structures that are observed in a real coastline under stormy conditions. Thus, the overall modelling approach appears to be a reliable resource to design and monitor the coastal environment. We are also developing a comprehensive database under a broad range of incident wind and wave conditions to predict overtopping rates. We have created a new Graphical User Interface (GUI) based on this database similar to the live online existing tool named Bayonet GPE available at <https://www.overtopping.co.uk/>, which is extensively used but unable to provide an answer for cases with wind speed. This ongoing GUI has been demonstrated through an animation in the project website, QatWeWos.org.uk, which will be updated regularly.

Acknowledgement

This project is funded and supported by the NERC and CIRIA (NE/R009155), to whom we are very grateful.

References

- Capitao, A.P. 2017. Description and validation of the rotorDiskSource class for propeller performance estimation. In: Proceedings of CFD with OpenSource Software.
- Chalikov, D., 1978. The numerical simulation of wind-wave interaction. Journal of Fluid Mechanics, Cambridge University Press, 87, 561-582.
- EurOtop, 2018. Manual on wave overtopping of sea defences and related structures. An overtopping manual largely based on European research, but for worldwide application. Van der Meer, J.W., Allsop, N.W.H., Bruce, T., De Rouck, J., Kortenhaus, A., Pullen, T., Schüttrumpf, H., Troch, P. and Zanuttigh, B., www.overtopping-manual.com.
- Hasan, S.A., Sriram, V., Paneer Selvam, R., 2018. Numerical modelling of wind-modified focused waves in a numerical wave tank. Ocean Engineering, Elsevier, 160, 276-300.
- Higuera, P., Lara, J.L., Losada, I.J., 2013. Realistic wave generation and active wave absorption for Navier-Stokes models application to OpenFOAM. Coastal Engineering, Elsevier, 71, 102-118.
- Isaacson, M., 1991. Measurement of regular wave reflection. Journal of waterway, port, coastal and ocean engineering, ASCE, 117(6), 553-569.
- Jacobsen, N.G., 2017. Waves2Foam manual.
- Jacobsen, N.G., Fuhrman, D.R., Fredsoe, J., 2012. A wave generation toolbox for the open-source CFD library: OpenFOAM. International journal for numerical methods in fluids, Wiley Online, 70(9), 1073-1088.
- Kharif, C., Giovanangeli, J.-P., Touboul, J., Grare, L., and Pelinovsky, E., 2008. Influence of wind on extreme wave events: experimental and numerical approaches. Journal of Fluid Mechanics, Cambridge University Press, 594, 209-247.
- Miles, J.W., 1957. On the generation of surface waves by shear flows. Journal of Fluid Mechanics, Cambridge University Press, 3, 185-204.
- Ward, D.L., Wibner, C.G. and Zhang, J. 1998. Runup on coastal revetments under the influence of onshore wind. Journal of Coastal Research, Coastal Education and Research Foundation, 14(4), 1325-1333.
- Ward, D.L., Zhang, J., Wibner, C.G., Cinotto, C.M., 1996. Wind effects on runup and overtopping. In: Proceedings of 25th Coastal Engineering conference. pp. 2206-2215.
- Xie, Z., 2014. Numerical modelling of wind effects on breaking solitary waves. European Journal of Mechanics B/Fluids, Elsevier, 43, 135-147.
- Yan, S., Ma, Q.W., 2010. Numerical simulation of interaction between wind and 2D freak waves. European Journal of Mechanics B/Fluids, Elsevier, 29, 18-31.